

Simulation of Quenching Process of Steels Creating Complex Carbides

Peter Fabian

Professor
University of Žilina
Faculty of Mechanical Engineering
Žilina,
Slovak Republic

Jozef Meško

Professor
University of Žilina
Faculty of Mechanical Engineering
Žilina,
Slovak Republic

Ružica R. Nikolić

Professor
University of Kragujevac
Faculty of Engineering
Kragujevac, Serbia
and
University of Žilina
Research Center
Žilina,
Slovak Republic

The scientific research, presented in this paper, deals with numerical modelling of the quenching process of conventional carbon steels. The developed numerical model simulates the quenching process of the hyper-eutectoid steels whose microstructure contains complex carbides. Those include the high-alloyed hyper-eutectoid steels intended for example for bearings, or high speed steel products. The calculation software SYSWELD, based on the finite element method, was used. The results of numerical modelling were compared with actual properties of quenched samples made of the hyper-eutectoid bearing steel. The microstructure was studied and hardness was measured in order to verify the numerical model's accuracy. The presented results indicate the absence of carbidic phase in the simulation calculations. This implies relatively large deviations in the simulated hardness results compared to reality. Those deviations must be considered in the case of simulating the microstructure and hardness of bearing steels using the SYSWELD software.

Keywords: quenching, numerical modelling, complex carbides, phase transformations, bearing steels.

1. INTRODUCTION

The possibility of modelling the quenching process brings an advantage in predicting the phase transformations in steel and its related microstructure, hardness and grain size. Mechanical analysis allows the prediction of deformations occurring during the quenching. In this manner, it is also possible to find out the values of stress generated in the material during quenching. The above method enables us to predict, in advance, whether a given material is suitable for the proposed type of heat treatment, whether it meets the specified parameters and whether it will be economically viable to process the given material to its required properties and purpose. Thus, the simulation serves the purpose of choosing the suitable parameters of quenching; however, it may also address the treatment of the component in view of its desired properties after quenching and elimination of crack formation during the quenching.

Numerous previous studies have laid the foundation for simulation of the phase transformations in steels. Initially, those studies dealt with the two-dimensional simulation. In particular, the studies published by authors [1-3] focused on modelling the phase transformations in steels, namely the two-dimensional modelling of austenite-pearlite eutectoid steels. The aforementioned studies did not include the diffusionless transformation that is significant for quenching. Over time, studies on modelling extended to the three-

dimensional modelling and post-quenching deformation modelling. Recent studies of quenching modelling, such as those by teams of authors [4, 5, or extensive studies by [6-8] have already dealt with modelling the diffusionless transformations in steel. However, those are related to conventional carbon steels whose structure prior to quenching consists of homogeneous austenite and after quenching it contains diffusionless transformation products such as martensite, bainite and residual, i.e. untransformed austenite.

The above methodology focuses on the issue of modelling the quenching of hyper-eutectoid steels that are not formed of homogeneous austenite in the austenitising temperature domain. During the heat treatment process, their structure features complex globular carbides of iron and alloying elements. Those are dissolved during the austenitising, depending on austenitising temperature and austenitising temperature holding time, thus increasing the proportion of carbon in austenite. With increasing the carbon content in austenite the hardness achieved after quenching increases as well, [9, 10]. Although the software designed to model steels contains a database of such steels' material properties, in the actual modelling, however, they are based on the assumption that these steels, similar to conventional carbon steels, are formed of homogeneous austenite prior to the immersion in the quenching medium.

This issue is the most pronounced in the form of a comparison between the modelled Vickers hardness and the actually achieved hardness.

2. HEAT TRANSFER MODELLING

Various processes occur during the quenching: heat transfer, phase transformations and mechanical inter-

Received: Novembar 2016, Accepted: February 2017

Correspondence to: Dr Ruzica Nikolic,
University of Zilina, Research Center
Zilina, Slovak Republic

E-mail: ruzicarnikolic@yahoo.com

doi:10.5937/fmet1704510F

© Faculty of Mechanical Engineering, Belgrade. All rights reserved

FME Transactions (2017) 45, 510-516 510

actions. The heat transfer is essentially a physical problem. The heat transfer in a component during the quenching can be described mathematically using an appropriate form of the Fourier heat conduction equation, considering the change of the temperature field in the form of the latent heat of phase transformations [8]:

$$\rho c \dot{T} = \nabla \cdot (\nabla (\lambda T)) + Q \quad (1)$$

where: ρ (kgm^{-3}) is the density, c (J K^{-1}) is the heat capacity, λ ($\text{Wm}^{-1}\text{K}^{-1}$) is the conductivity of a mixture of phases in terms of temperature, and Q (J) is the internal heat source in the form of the latent heat that is a function of temperature and cooling intensity.

The heat conduction and the internal heat source in the latent heat form can be described by equation [5]:

$$\frac{\partial}{\partial x} \left(k \frac{\partial T}{\partial x} \right) + \frac{\partial}{\partial y} \left(k \frac{\partial T}{\partial y} \right) + \frac{\partial}{\partial z} \left(k \frac{\partial T}{\partial z} \right) + \dot{q} = \rho C_p \frac{\partial T}{\partial t} \quad (2)$$

where: T ($^{\circ}\text{C}$) is the temperature, t (s) is the time, while C_p (JK^{-1}) is the specific heat, k ($\text{Wm}^{-1}\text{K}^{-1}$) is the thermal conductivity and \dot{q} is the latent heat allocation from the phase transformations.

The thermo-physical properties of steels are functions of two parameters – temperature and volume fraction of transformed phases. Those can be calculated using the following equation [5]:

$$k^j = \sum X_i^j k_i^j, C_p^j = \sum X_i^j C_{pi}^j \quad (3)$$

where k_i^j ($\text{Wm}^{-1}\text{K}^{-1}$) is the thermal conductivity, C_{pi}^j ($\text{Jkg}^{-1}\text{K}^{-1}$) is the specific heat capacity and X_i^j is the volume fraction of the i -th phase at the j -th time.

During the cooling of steel the latent heat is generated, which is caused by phase transformations. This phenomenon is included in the modelling as follows [5]:

$$\dot{q} = \Delta H_i \frac{\Delta X_i}{\Delta t} \quad (4)$$

where ΔH_i (J) is the amount of heat released at the temperature T_i (K) and ΔX_i is the amount of phase transformations that have taken place during the interval Δt (s).

The component austenitising temperature T_0 (K) was considered as the initial state. It was assumed that this temperature is uniform throughout the component volume. In this case, the boundary condition is as follows [5, 11]:

$$-k \frac{\Delta T}{\Delta n} = h(T_s - T_A), \quad (5)$$

where: n is the surface outer boundary, h ($\text{Wm}^{-2}\text{K}^{-1}$) is the convective heat transfer coefficient, T_s ($^{\circ}\text{C}$) is the surface temperature, and T_A ($^{\circ}\text{C}$) is the ambient temperature.

3. MODELLING DIFFUSION AND DIFFUSIONLESS PHASE TRANSFORMATION

When modelling the phase transformations one starts from the basic assumption that the microstructure

develops in different ways depending on the temperature, cooling rate and carbon content, [2, 12]. In order to predict the volume fraction of individual phases during the quenching – austenite, ferrite, pearlite and martensite – one can describe the diffusion and diffusionless transformation models according to Figure 1 that shows a schematic IRA diagram of eutectoid steel. The kinetics of a diffusion transformation from the assumed isothermal curve can be described by equation [2]:

$$F_i = 1 - \exp(-At_j^B) \quad (6)$$

where: F_i is the volume fraction of the i -th phase during the phase transformation. Material properties A and B can be determined directly from the IRA diagram. The transformation time t_j was transferred to the sum of the time period and the time was obtained from the volume fraction of each phase in the previous time step F^{j-1} of the simulation. It can be written as [2]:

$$t_j = \Delta t_j + \left\{ -\frac{\ln(1 - F^{j-1})}{A} \right\}^{\frac{1}{B}} \quad (7)$$

However, the process of anisothermal transformation cannot be described using equations (6) and (7). Therefore, it is necessary to apply the Scheil's rule [8] on the cooling curve division into small time periods, as shown in Figure 1. The transformation is considered to have started when the following equation is satisfied [2, 13]:

$$\sum_{j=1}^m \frac{\Delta t_j}{\tau_j} = 1 \quad (8)$$

where: τ_j (s) is the time of the transformation start at the j -th time of the simulation.

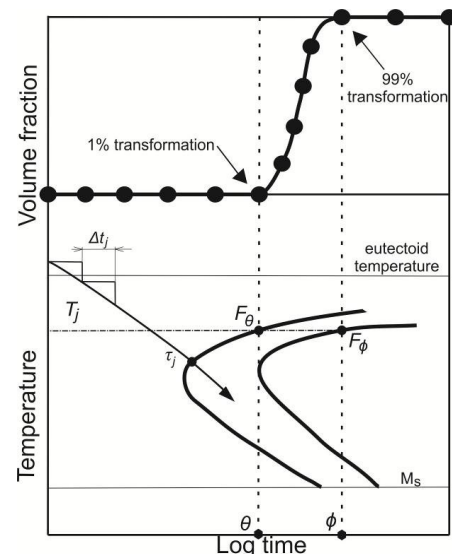


Figure 1. The schematic IRA diagram and graphical dependence of the structure volume fraction [2].

A diffusionless transformation that is independent of time can be empirically described by a model derived from experiments, [14].

This means that the amount of martensite can be fully expressed as a function of temperature as follows:

$$F_m = [1 - \exp\{-0,011(M_s - T)\}] \cdot \left(1 - \sum_i F_i\right) \quad (9)$$

where F_m is the volume fraction of martensite, and F_i is the volume fraction of other phases, M_s is the temperature of the martensitic transformation start; and T is the ambient temperature. Since the ferrite and pearlite are austenitic transformation products and are they not transformed into martensite, the equation

includes the segment $\left(1 - \sum_i F_i\right)$.

The latent heat that is generated during the transformation increases the temperature in the material. This internal heat source is related to enthalpy change, and the three types of enthalpy forms are considered:

- transformation to ferrite,
- transformation to pearlite,
- transformation to martensite.

The component austenitising temperature is generally high above the boiling point of the quenching medium. During the quenching, the cooling process is characterized by three phases:

- steam cushion,
- boiling and
- convection,

each being associated with a significant change in cooling. At the same time it is necessary to take into account the initial phase as well, when there is a contact of the cooled component with the liquid. The critical phases of the heat flux and heat transfer are illustrated in Figure 2.

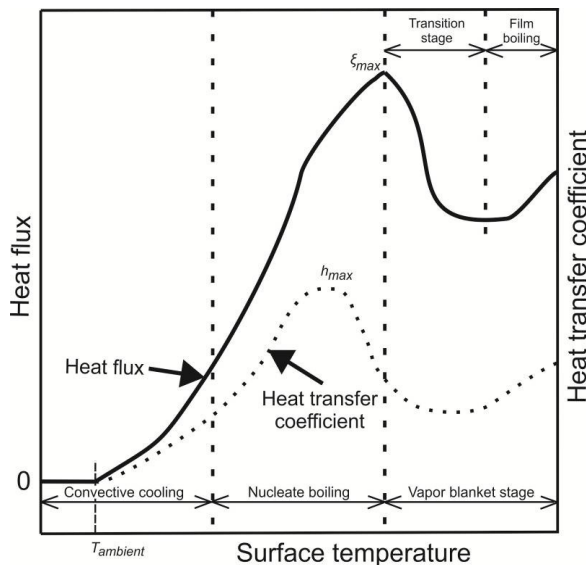


Figure 2. Change in the heat flux and heat transfer coefficient in terms of temperature and cooling phase [14].

4. HARDNESS MODELLING

Prediction of hardness in the modelled component volume uses the application of Maynier's model, [15, 16]. The equation takes into account the impact of the steel chemical composition and of the cooling rate on the hardness of individual phases:

$$HV_M = 127 + 949C + 27Si + 11Mn + 8Ni + 16Cr + 21 \log V_r \quad (10)$$

$$HV_B = 323 + 185C + 330Si + 153Mn + 65Ni + 144Cr + 191Mo + (89 + 53C - 55Si - 22Mn - 10Ni - 20Cr - 33Mo) \log V_r \quad (11)$$

$$HV_{F+P} = 42 + 223C + 53Si + 30Mn + 12.6Ni + 7Cr + 19Mo + (10 - 19Si + 4Ni + 8Cr + 130V) \log V_r \quad (12)$$

where: HV_M , HV_B and HV_{F+P} are the Vickers hardness of martensite, bainite and a mixture of ferrite and pearlite, respectively. The weight of alloying elements in the steel is indicated in (%), and V_r ($^{\circ}\text{Ch}^{-1}$) is the cooling rate at 700°C .

The total hardness of each component is then calculated according to the following formula:

$$HV = X_M HV_M + X_B HV_B + (X_F + X_P) HV_{F+P}, \quad (13)$$

where: X_M , X_B , X_F and X_P are the volume fractions of martensite, bainite, ferrite and pearlite, respectively.

5. EXPERIMENTAL MATERIAL

From the selected group of steels, whose microstructure contains complex carbides the bearing steel 100Cr6 with chemical composition shown in Table 1, was chosen.

Table 1. Chemical composition of the experimental bearing steel 100Cr6

Element	C	Si	Mn	Ni	Cr	Mo
%	0.93	0.28	0.42	0.04	1.54	0.03

In the given case, one is dealing with the bearing steel for bearing rings of a smaller wall thickness and bearing bodies up to 25 [mm] diameter. This steel is easily machinable in the soft annealed state. The initial microstructure, prior to quenching, should be formed of fine globular carbides uniformly distributed in the ferritic matrix (the so-called globular pearlite).

The standard bearing steel heat treatment is quenching and low-temperature tempering. The diagram of anisothermal austenite decay (Figure 3) clearly shows that pearlitic, bainitic and martensitic transformations may occur in this steel while cooling. In technological practice of bearing component quenching, one is trying to avoid the pearlitic and, to the maximum extent possible, the bainitic transformations, as well. The resulting microstructure contains lath martensite, a reasonable amount of residual austenite and carbidic phase.

6. SIMULATION AND INPUT PARAMETERS

The simulation was carried out for a selected set of bearing rings made of 100Cr6 steel, in order to predict the resulting microstructure and hardness after quenching. Figure 4 shows the bearing rings dimensions.

The simulation was performed using the commercial software SYSWELD 2010, and the bearing ring model was created in VISUAL MESH 6.5. Due to the axial symmetry of bearing rings, it was sufficient to perform the above simulation for half of the bearing ring only, respectively for a 2-D section surface.

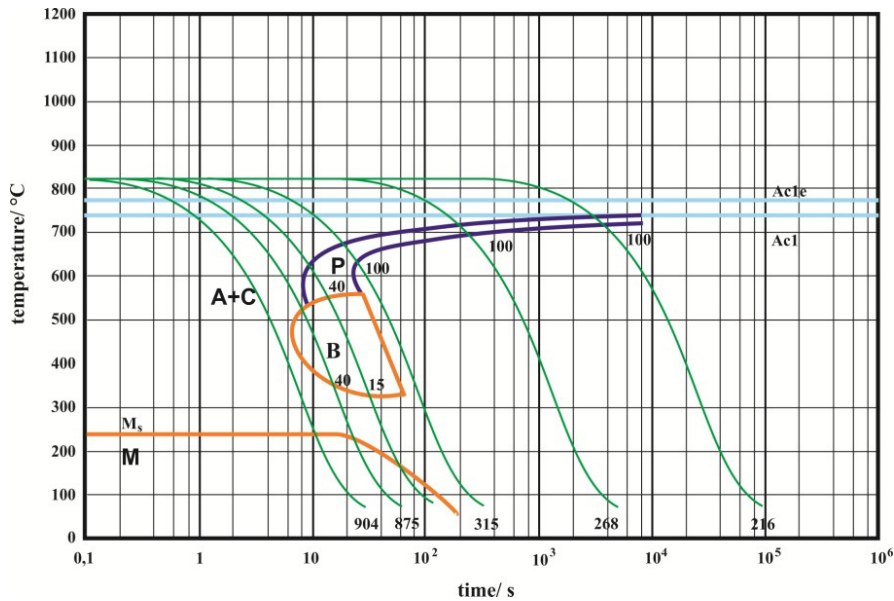


Figure 3. The ARA diagram of bearing steel 100Cr6 [9]

However, since the entire research also focuses on simulating stress and deformations in bearing rings during the quenching, the model was created of the whole profile.

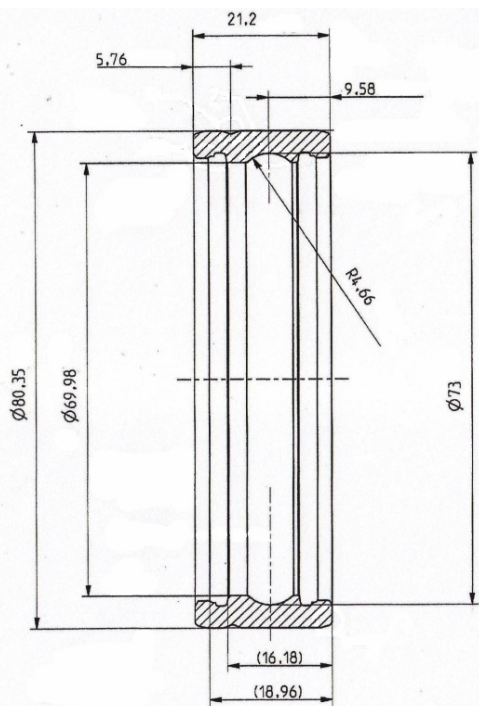


Figure 4. Scheme of the experimental bearing ring [mm]

The creation of a bearing ring model consisted of exporting the bearing ring wall section to VISUAL MESH software, creating a network of nodal points on this surface and creating a rotated 3-D mesh of these nodes. The distance between the individual layers was smaller on the model surface that was to be in contact with the cooling medium (0.1 [mm]) and larger in the core (0.5 [mm]). The mesh itself was created using the Quad-Tria method. Those points formed the volume to be cooled down. That volume's envelope was defined for the heat transfer from the component to the medium (Figure 5).

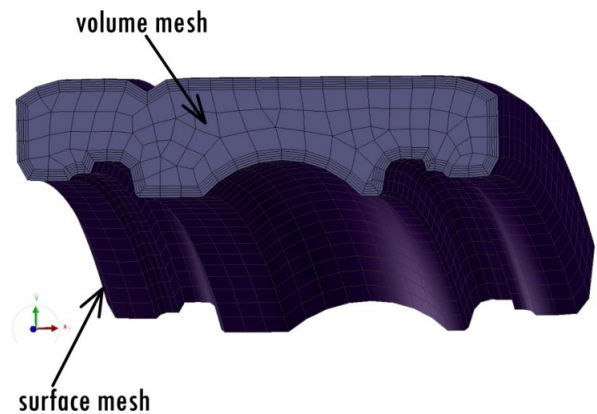


Figure 5. Principles of creating a model of an experimental bearing ring

The bearing ring simulation was carried out for three austenitising modes. Their length was always 20 minutes, but they differed in the austenitising temperature used. The first simulation was carried out for austenitising at 830°C, the second one for austenitising at 850°C and the third one for austenitising at 870°C. In addition to duration, the austenitising temperature is the second main parameter that determines the dissolution of the carbidic phase in austenite. With increasing the austenitising temperature, the share of carbon increases as well. That carbon is released from the carbidic phase into the austenite, until it reaches the maximum possible value.

Cooling was carried out in the mineral quenching oil DURIXOL W72 immediately after 20 minutes held at the austenitising temperature. The mineral oil temperature was 20°C.

7. DISCUSSION OF RESULTS

Figure 6 clearly shows how the bearing rings cooling took place after immersion in mineral quenching oil. Two seconds after the bearing rings were immersed in mineral oil the difference between their surface and the core temperatures was approximately 400°C.

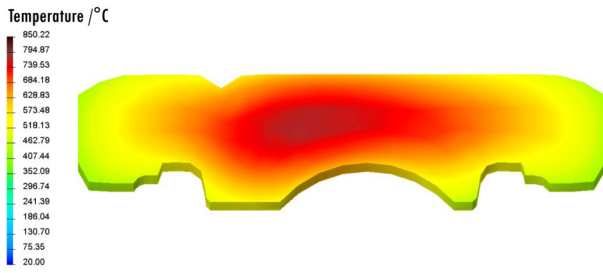


Figure 6. Temperature reading in the bearing ring cross section two seconds after immersion in mineral oil

Before comparing the achieved and simulated microstructures, it must be emphasized that the simulation software does not take into account the carbidic phase in steels. The simulation assumes that the microstructure of the cooled component, prior to immersion in the cooling medium (i.e. prior to heat dissipation), is formed of homogenous austenite throughout its volume (Figure 7).

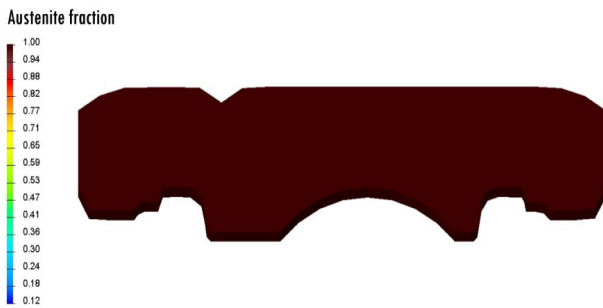


Figure 7. Microstructure of bearing rings just before immersion in mineral oil (according to the simulation)

After completion of cooling, according to the simulation, the bearing ring microstructure for the three austenitising modes consisted of 88% martensite and 12% residual austenite (Figures 8 and 9).



Figure 8. Share of martensite in the bearing ring microstructure after quenching (according to the simulation)

The microstructures obtained after quenching essentially differ only in the size of the carbidic phase. The largest carbides were found in the structure austenities at the lowest temperature (830°C); on the other hand, the smallest carbides were found in the microstructure austenities at the highest temperature (870°C). The microstructure consisted of the lath martensite, residual austenite and carbidic phase.

The results of bearing ring microstructure simulation after quenching represent a basis for simulating the most technologically important parameter – hardness. According to the simulation, the hardness after quenching throughout the cross section of bearing rings was virtually identical, i.e. 784 [HV], (Figure 10).

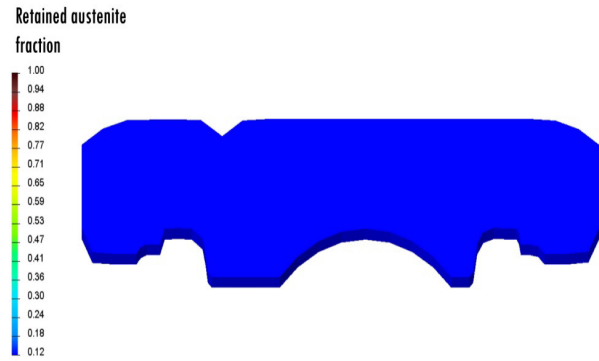


Figure 9. Share of residual austenite in the bearing ring microstructure after quenching (according to the simulation)



Figure 10. Hardness in the cross section of bearing rings after quenching (according to the simulation)

To verify the simulation results of bearing ring hardness after quenching, the hardness measurements using the HV1 Vickers method, as shown in the scheme in Figure 11, were carried out. Figure 12 shows the results of Vickers hardness measurement for all the three-austenitising modes.

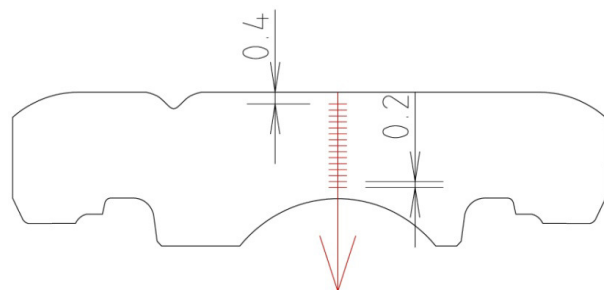


Figure 11. Scheme of hardness measurement in the bearing rings cross sections [mm]

The graphic representation of the hardness measurement results for individual austenitising mode clearly shows that the simulation software approached the true values of hardness only in the case of austenitising at the lowest temperature of 830°C. That temperature is very rarely used in technical practice (Figure 12a), although the hardness curve in the bearing ring cross section was not even captured here.

Deviations in the most frequently used austenitising temperature – 850°C (Figure 12b) – were already significant (approximately 120 [HV]).

In the case of the highest used austenitising temperature – 870°C (Figure 12c) – the deviations were logically the largest (approximately 140 [HV]), due to the largest share of carbon received by austenite from the dissolved carbidic phase.

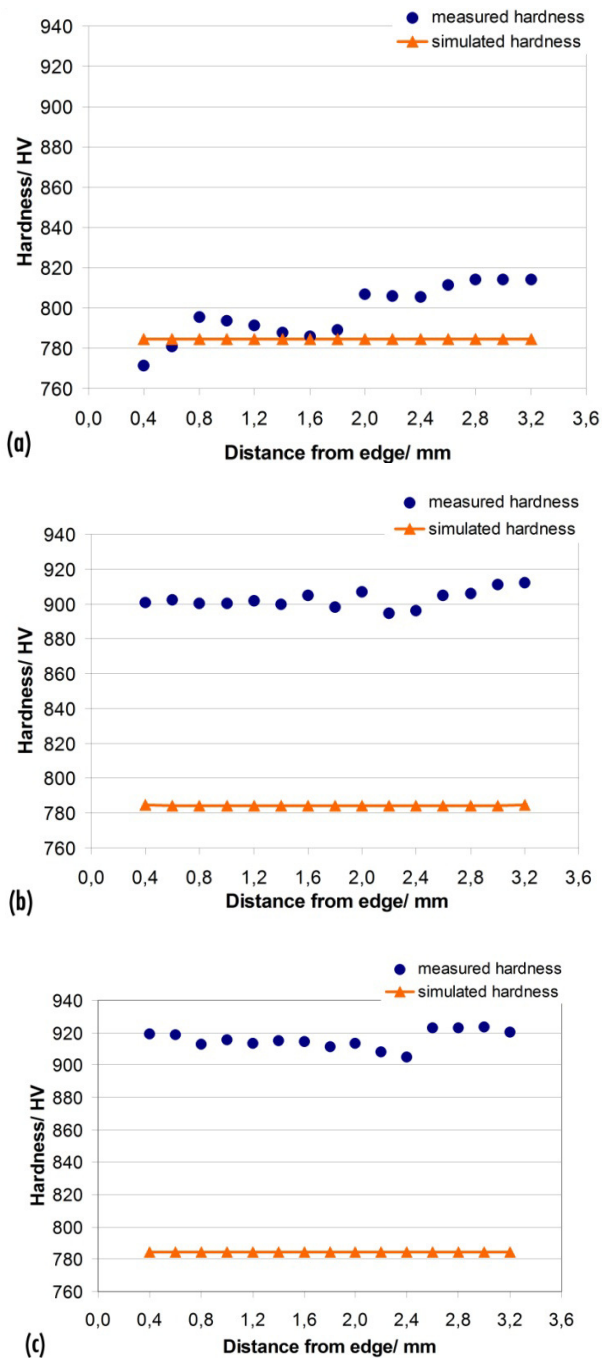


Figure 12. Measured hardness values after simulation and actual quenching: (a) $A_{Cm} = 830^{\circ}C$; (b) $A_{Cm} = 850^{\circ}C$; (c) $A_{Cm} = 870^{\circ}C$,] with a holding time $t = 20$ [min].

8. CONCLUSIONS

This paper analyzed the possibility of modelling the thermal-metallurgical parameters of steels forming the carbide phase in the microstructure.

In this case, the subject of research were the hyper-eutectoid steels alloyed with chromium carbide formers. The complex carbides $(Fe, Cr)_3C$ were dissolved in austenite depending on the temperature and holding time at that temperature.

The presented results indicate the absence of carbide phase in the simulation calculations. This implies relatively large deviations in the simulated hardness results compared with reality.

At the austenitising temperatures of $850^{\circ}C$ and $870^{\circ}C$ carbon gets into austenite at a significantly greater extent than at the temperature of $830^{\circ}C$, therefore the differences between the simulation and reality are not so small.

Those deviations must be considered in the case of simulating the microstructure and hardness of bearing steels using the SYSWELD software.

ACKNOWLEDGMENT

Research presented in this paper was partially supported through realization of the projects KEGA no. 054 ŽU – 4/2012 and VEGA no. 1/0186/09; project "Research Center of the University of Žilina" - ITMS 26220220183 financed by the European regional development fund and the Slovak state budget by the project and grants TR35024 and ON174004 financed by the Ministry of Education, Science and Technological Development of Republic of Serbia.

REFERENCES

- [1] Mesko, J., Fabian, P., Hopko, A., Konar, R.: Shape of heat source in simulation program SYSWELD using different types of gases and welding methods, Eng. Techn., Vol. XVI, No. 5, pp. 6-11, 2011.
- [2] Denis, S., Farias, D., Simon, A.: Mathematical model coupling phase transformations and temperature evolutions in steels, ISIJ International, Vol. 32, No. 3, pp. 316-325, 1992.
- [3] Sejc, P. et al.: Computer simulation of heat affected zone during MIG brazing of zinc – coated steel sheets, Kovové materiály - Metallic materials, Vol. 44, No. 4, pp. 225-234, 2006.
- [4] Breznican, M., Fabian, P., Mesko, J., Drbul, M.: The simulation of influence of quenching temperature on properties of bearing rings, Manuf. Techn., Vol. 13, No. 1, pp. 20-25, 2013.
- [5] Kang, S.H., Im, Y.T.: Thermo-elasto-plastic finite element analysis of quenching process of carbon steel, J. Mat. Proc. Techn., Vol. 192-193, pp. 381-390, 2007.
- [6] Novak, P. et al: Finite element implementation of multi-pass fillet weld with phase changes, Manuf. Techn., Vol. 13, No. 1, pp. 79-85, 2013.
- [7] Zmindak, M., Novak, P., Mesko, J.: Numerical simulation of arc welding processes with metallurgical transformations, Metalurgija - Metallurgy, Vol. 49, No. 2, pp. 595-599, 2010.
- [8] Gur, C.H., Pan, J.: *Handbook of Thermal Process of Steels*, CRC Press, London, 2008.
- [9] Bhadeshia, H.: *The theory and significance of retained austenite in steels*, PhD. Thesis, University of Cambridge, UK, 1979.
- [10] Zmindak, M., Radziszewski, L., Pelagic, Z., Falat, M.: FEM/BEM techniques for modeling of local fields in contact mechanics, Communications, Vol. 17, No. 3, pp. 37-46, 2015.
- [11] Pastorek, P., Pelagic, Z., Zmindak, M.: FEM analysis stresses in dynamic contact problems, in:

Proceedings of XI International Conference Dynamics of rigid and deformable bodies, 9.-11.10.2013, Ústí nad Labem, CD-ROM, pp. 1-8. (ISBN 978-80-7414-607-7).

- [12] Fabian, P. et al.: Simulation of roundness, hardness and microstructure of bearing rings with thin cross sections by using SYSWELD, Communications, Vol. 16, No. 3A, pp. 124-129, 2014.
- [13] Jankejech, P., Fabian, P., Kyselova, M.: Application of Barkhausen noise on the surface integrity of bearing components, Wulfenia J., Vol. 21, No. 4, pp. 503-514, 2014.
- [14] Kostinen, D.P., Marburger, R.E.: A General Equation for Austenite – Martensite Transformation in Pure Carbon Steels, Acta Metall., Vol. 7, pp. 59-60, 1959.
- [15] Trzaska, J. et al.: The calculation of CCT diagrams for engineering steels, Arch. Mat. Sci. Eng., Vol. 39, No. 1, pp. 13-20, 2009.
- [16] Sejc, P.: *Protective gasses in welding* (Ochranné plyny vo zváraní), STU Bratislava, 2002. (In Slovak).

**СИМУЛАЦИЈА СТВАРАЊА СЛОЖЕНИХ
КАРБИДА ТОКОМ КАЉЕЊА ЧЕЛИКА**

П. Фабијан, Ј. Мешко, Р. Николић

Научно истраживање, представљено у овом раду, се бави нумеричким моделирањем процеса каљења конвенционалних угљеничних челика. Развијен нумерички модел симулира процес каљења хипер-еутектоидних челика чија микроструктура садржи сложене карбиде. Ово укључује високо-легиране хипер-еутектоидне челике који су намењени, на пример, за лежајеве или делове који раде при великим брзинама. Коришћен је рачунски софтвер SYSWELD, који је заснован на промени методе коначних елемената. Резултати нумеричког моделирања су упоређени са стварним својствима каљених узорака, који су направљени од хипер-еутектоидног челика за лежајеве. Проучавана је микроструктура и тврдоћа је мерена да би се верификовала тачност нумеричког модела. Представљени резултати показују одсуство карбидне фазе у симулационом прорачуну. Ово имплицира релативно велика одступања резултата тврдоће добијене симулацијом и стварних вредности. Ова одступања се морају узети у обзир у случајевима симулације микроструктуре и тврдоће челика за лежајеве коришћењем софтвера SYSWELD.